

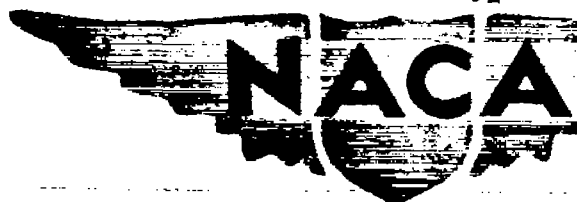
RM No. E7B01

MAY 8 1947

C2

6960

GEI-1014



RESEARCH MEMORANDUM

FUEL TESTS ON AN I-16 JET-PROPULSION ENGINE

AT STATIC SEA-LEVEL CONDITIONS

By Ray E. Bolz and John B. Meigs

Aircraft Engine Research Laboratory
Cleveland, Ohio

CLASSIFIED DOCUMENT

This document contains classified information affecting the National Defense of the United States within the meaning of the Espionage Act, USC 50:31 and 32. Its transmission or the revelation of its contents in any manner to an unauthorized person is prohibited by law. Information so classified may be imparted only to persons in the military and naval Services of the United States, appropriate civilian officers and employees of the Federal Government who have a legitimate interest therein, and to United States citizens of known loyalty and discretion who of necessity must be informed thereof.



NATIONAL ADVISORY COMMITTEE FOR AERONAUTICS

WASHINGTON

April 29, 1947

N A C A LIBRARY

LANGLEY MEMORIAL AERONAUTICAL
LABORATORY
Langley Field, Va.

unclassified



NATIONAL ADVISORY COMMITTEE FOR AERONAUTICS

RESEARCH MEMORANDUM

FUEL TESTS ON AN I-16 JET-PROPULSION ENGINE

AT STATIC SEA-LEVEL CONDITIONS

By Ray E. Bolz and John B. Meigs

SUMMARY

The effect of fuel composition and boiling point on the performance of the type I-16 jet-propulsion engine was investigated.


Tests were made on 14 fuels embodying different types of hydrocarbon and having boiling points lying within the range of 150° to 650° F. Each fuel was tested in an I-16 engine at static sea-level conditions at 13 rotor speeds varying from 11,000 to 16,500 rpm. Performance was based on speed, thrust, fuel flow, air flow, tail-pipe temperature and pressure, and temperature rise and pressure drop across the combustion chamber.

The results show that for the I-16 engine tested at static sea-level conditions:

Fuel composition and boiling range have a negligible effect upon engine thrust, rotor speed, and gas temperatures for the principal types of hydrocarbon fuel when used for short periods of time. The effect of fuel types on the performance and reliability of the engine over long periods of operation was not determined. Operation of the engine using fuels containing very high percentages of aromatics and olefins resulted in visible black smoke in the exhaust gases. The smoke from the aromatics was much more dense than that resulting from the olefinic fuel.

INTRODUCTION

A program to investigate the effect of fuel composition and volatility on jet-propulsion-engine performance and to obtain data that may be useful for establishing effective jet fuel specifications is being conducted at the NACA Cleveland laboratory. As part of this program, 14 fuels were investigated including hydrocarbons of the paraffin, naphthene, aromatic, and olefin classes. The fuels



were also selected to represent a wide boiling range, 150° to 650° F, in order that the effect of boiling point as well as fuel composition on the performance of the I-16 engine at static sea-level operation might be determined. The selection of fuels was limited by the necessity of choosing only fuels readily obtainable in sufficient quantity. Performance was based on engine thrust, fuel flow, air flow, tail-pipe temperature, tail-pipe pressure, temperature rise across the combustion chamber, and pressure drop across the combustion chamber. The effect of the fuels on engine life, engine starting performance, and carbon deposits was not investigated.

EQUIPMENT


The general arrangement of the test-engine installation in the test cell is shown in figure 1. The I-16 jet-propulsion engine, tail pipe, and nozzle were rigidly mounted on a floating framework suspended from the ceiling of the test cell by four rods connected to ball-bearing pivots. Four guide rollers were used to restrain lateral motion of the floating frame assembly. The tail pipe of the engine extended through the test cell. A seal in the wall of the test cell minimized air leakage into the room without restricting the longitudinal movement of the assembly. All fuel lines and manometer leads were joined to the engine by rubber-hose connections to provide flexibility.

The test cell itself was a large reasonably airtight chamber. The air supply to the engine entered the test chamber through an 18-inch A.S.M.E. standard metering nozzle. The air leakage into the cell was measured and included in the calculations of the air flow to the engine.

Figure 1 also shows the mechanism for measuring static thrust. In this instrument the thrust exerted by the suspended engine was transferred by the crank-lever arrangement to a diaphragm in an air chamber. The thrust was indicated by a manometer connected to the air chamber and the manometer readings were converted into pounds thrust by means of a dead-weight calibration of the thrust meter.

A rotameter was used for measuring rate of fuel flow and was calibrated for each fuel tested. A chronometric tachometer measured the rotor speed and Bourdon gages indicated lubricating-oil pressures, fuel-supply pressure, and fuel-nozzle pressure.

The location of the thermocouples and pressure tubes in the I-16 engine is shown in figure 2. Iron-constantan thermocouples were distributed around the front and rear compressor inlets and thermocouples



were placed in the compressor-outlet elbows leading to combustion chambers 4 and 9. Seven shielded total-pressure tubes in the expansion joint just back of the compressor outlet gave a survey of the total pressure of the air entering the combustion chamber. Three total-pressure tubes (fig. 3(a)) and three shielded thermocouples (fig. 4(a)) were installed in the exit of combustion chambers 4 and 9. An integrating total-pressure rake (fig. 3(b)) and seven shielded thermocouples (fig. 4(b)), both in an equal-area traverse, were placed in the tail pipe at the nozzle entrance. The thermocouples used in the high-temperature and high-velocity gas streams were designed to minimize radiation and conduction losses. No attempt has been made, however, to compensate for the inability of the thermocouples to convert 100 percent of the kinetic energy of the gases into thermal energy.

FUELS

Data on physical properties and approximate chemical composition of the test fuels are given in table I. Solvent 1 and solvent 2 are two commercial hydrocarbon solvents that correspond roughly to two kerosene cuts with the aromatic hydrocarbons removed. Hot-acid octane, diisobutylene, methylcyclohexane, and benzene are representatives of the four general classes of hydrocarbons boiling in the gasoline range. Benzene, xylene, cumene, and solvent 3 (a commercial varnish solvent) are aromatics with different boiling ranges from 170° to 408° F. Hastings naphtha and Wood River olefinic stock are rich in naphthenes and olefins, respectively.

TEST PROCEDURE

The standard test for each of the 14 fuels consisted of runs at 10 consecutively increasing speeds ranging from 11,000 to 16,500 rpm, which is the rated speed of the rotor. The speed of 11,000 rpm was selected because it was the lowest speed at which the necessary fuel-manifold pressure could be obtained. About 20 minutes were required for each test.

Three check runs at decreasing speeds were also made for each fuel. A reference test was run each test day using solvent 1 from a single batch. These reference tests indicate that there was no change in engine operation from day to day other than the normal experimental deviation, which averaged about 3 percent with a maximum of about 5 percent.

RESULTS AND DISCUSSION

The performance data obtained in the fuel tests were all corrected to standard sea-level conditions at the engine inlet and the corrected values were used throughout in this paper.

The over-all performance of the I-16 jet engine when operated at static conditions and at sea level using the 14 fuels is shown in figures 5 to 9. Figure 5 shows the measured thrust exerted by the engine plotted against the heat input per hour, that is, the fuel flow multiplied by the lower heating value of the fuel. The use of heat input instead of fuel flow as the basis for comparison eliminates heating value as a variable. The results shown in figure 5 indicate that the effect of either fuel composition or boiling point on the performance of the engine at static sea-level conditions is negligible. The spread of the data (a maximum of about 6 percent) cannot be attributed to the differences in fuels because the spread in the daily check curves for solvent 1 is of the same magnitude. The solvent 1 check runs taken over the entire test period are shown in figure 6.

Figure 7 presents the rotor speed plotted against heat input for the 14 fuels. This curve again indicates the negligible effect of fuel composition or boiling point on engine performance. The variation in these data is a maximum of 3 percent, which also checks the variation in the data from the check runs on solvent 1 shown in figure 8. The speed data are more accurate than the thrust data because the instruments for measuring speed are more accurate.

Engine calibration curves of speed against thrust and speed against air flow plotted for all the fuels (figs. 9 and 10) indicate that over the period of the investigation the engine characteristics were constant.

Values of tail-pipe temperatures (fig. 11) and total pressures (fig. 12) were used to calculate the engine thrust; a 95-percent nozzle efficiency was assumed. The values of the calculated thrust checked the values of the measured thrust within 1 percent over the entire operating range and indicated good agreement among the thrust, temperature, and pressure measurements. The data in figures 11 and 12 further support the result that no measurable difference in engine performance occurred for the fuels tested.

Figure 13 shows both the thrust specific fuel consumption and the fuel-air ratio for each fuel tested (corrected to a standard

heating value of 19,000 Btu/lb) plotted against the rotor speed. Each of these factors is a ratio of two measured quantities and as such is subject to the combined error.

The average temperature rise in two combustion chambers as determined by the chromel-alumel thermocouples (fig. 4(a)) in the turbine inlet and the chamber inlet is shown in figure 14 for three fuels. The thermocouples in the turbine were difficult to maintain and for many of the runs one or two of the three thermocouples were inoperative. For the tests using the three fuels shown plotted in figure 14, all three thermocouples in the turbine entrance were operative. The data indicate a very high combustion efficiency (between 96 and 100 percent) over the range of fuel flow and concomitant rotor speeds tested. The accuracy of the data depends on how well the temperature at the combustion-chamber exit is represented by the three thermocouple readings taken.

Figure 15 shows the combustion-chamber total-pressure drop in percentage of chamber-inlet total pressure to the chamber plotted against speed. The curve shows a constant percentage pressure drop with an increase in engine speed, which, of course, means that the pressure of the air at the inlet to the combustion chamber increased with speed at about the same rate as did the pressure loss in the chamber. This pressure loss is the sum of the frictional pressure drop, which increases with density and velocity, and the momentum pressure drop, which increases with inlet velocity and fuel-air ratio.

The variation of combustion-chamber inlet total pressure with rotor speed is also shown in figure 15. From this curve the pressure ratio of the compressor at an engine speed of 16,000 rpm was computed to be 3.47.

Observation of the exhaust gas during engine operation showed that only the use of aromatic fuels (benzene, xylene, cumene, and the highly aromatic solvent 3) and the olefinic fuel (diisobutylene) resulted in heavy smoke in the exhaust. The smoke formed from the aromatics was much more dense than that formed from the olefinic fuel. Tests indicated that a minimum of about 30 percent aromatics in a nonaromatic fuel was necessary to cause traces of visible smoke. The smoking tendency of fuels discussed had no effect on the thrust or efficiency of the engine during the short tests of approximately 20 minutes.

SUMMARY OF RESULTS

The data show that for the I-16 jet-propulsion engine tested with 14 different fuels at static sea-level conditions:

1. Fuel composition and boiling range had a negligible effect upon engine thrust, rotor speed, and gas temperatures for the principal types of hydrocarbon fuel when used for short periods of time. The effect of fuel types on the performance and reliability of the engine over long periods of operation was not determined.

2. Operation of the engine using fuels containing very high percentages of aromatics and olefins resulted in visible black smoke in the exhaust gases. The smoke from the aromatics was much more dense than that resulting from the olefinic fuel.

Aircraft Engine Research Laboratory,
National Advisory Committee for Aeronautics,
Cleveland, Ohio.

TABLE I - PHYSICAL DATA AND APPROXIMATE COMPOSITION OF FUELS TESTED IN I-16 JET ENGINE

Fuel	Boiling range (°F)	Specific gravity	Hydrogen-carbon ratio	Lower heating value (Btu/lb)	Approximate composition (percent by volume)			
					Paraffin	Naphthene	Aromatic	Olefin
Hot-acid octane ^a	174-257	0.715	0.188	19,200	100			
Diisobutylene ^a	210-216	.726	.167	19,000				100
Methylcyclohexane ^a	207-212	.773	.170	18,500		100		
Benzene ^{a b}	170-175	.883	.084	17,400			100	
Xylene ^b	273-278	.867	.106	17,600			100	
Cumene ^b	293-349	.863	.113	17,800			100	
Solvent 3 ^b	337-408	.881	.121	17,800			90	
62-octane gasoline	113-233	.699	.182	19,000	76	22	2	Low
Hastings naphtha	139-318	.756	.170	18,700		80-90	5	Low
Wood River olefinic stock	201-620	.819	.171	18,750				30
Kerosene	302-488	.809	.164	18,500	45	25	28	2
Solvent 1	307-382	.769	.174	18,800	62	36	2	Low
Solvent 2	370-485	.792	.174	18,700	62	33	5	Low
Diesel fuel oil	350-655	.829	.161	18,400			40	

^aFuels in gasoline boiling range representing the four classes of hydrocarbons.

^bAromatic fuels with various boiling ranges.

National Advisory Committee
for Aeronautics

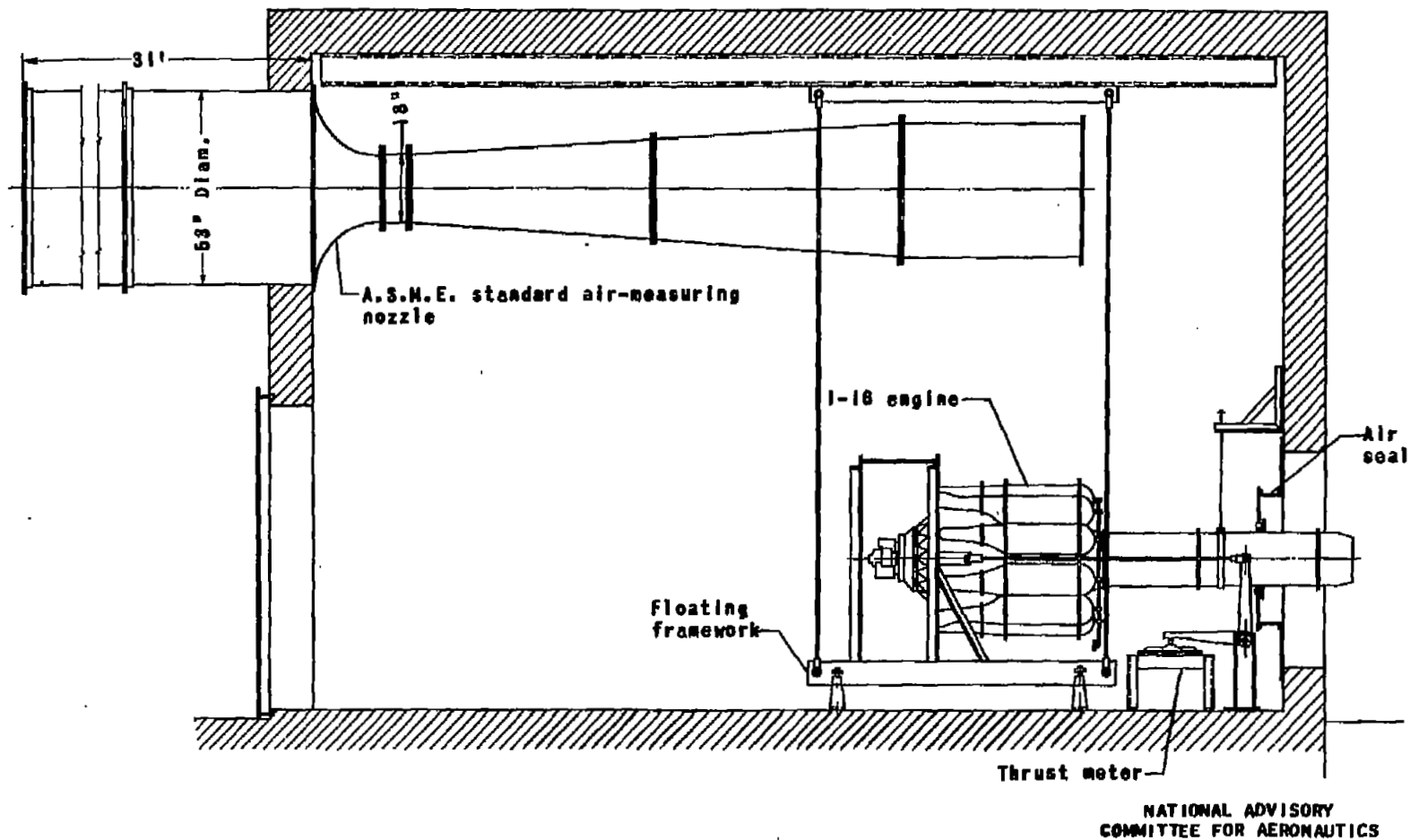


Figure 1. - General arrangement of the J-16 jet-propulsion engine in the test cell.

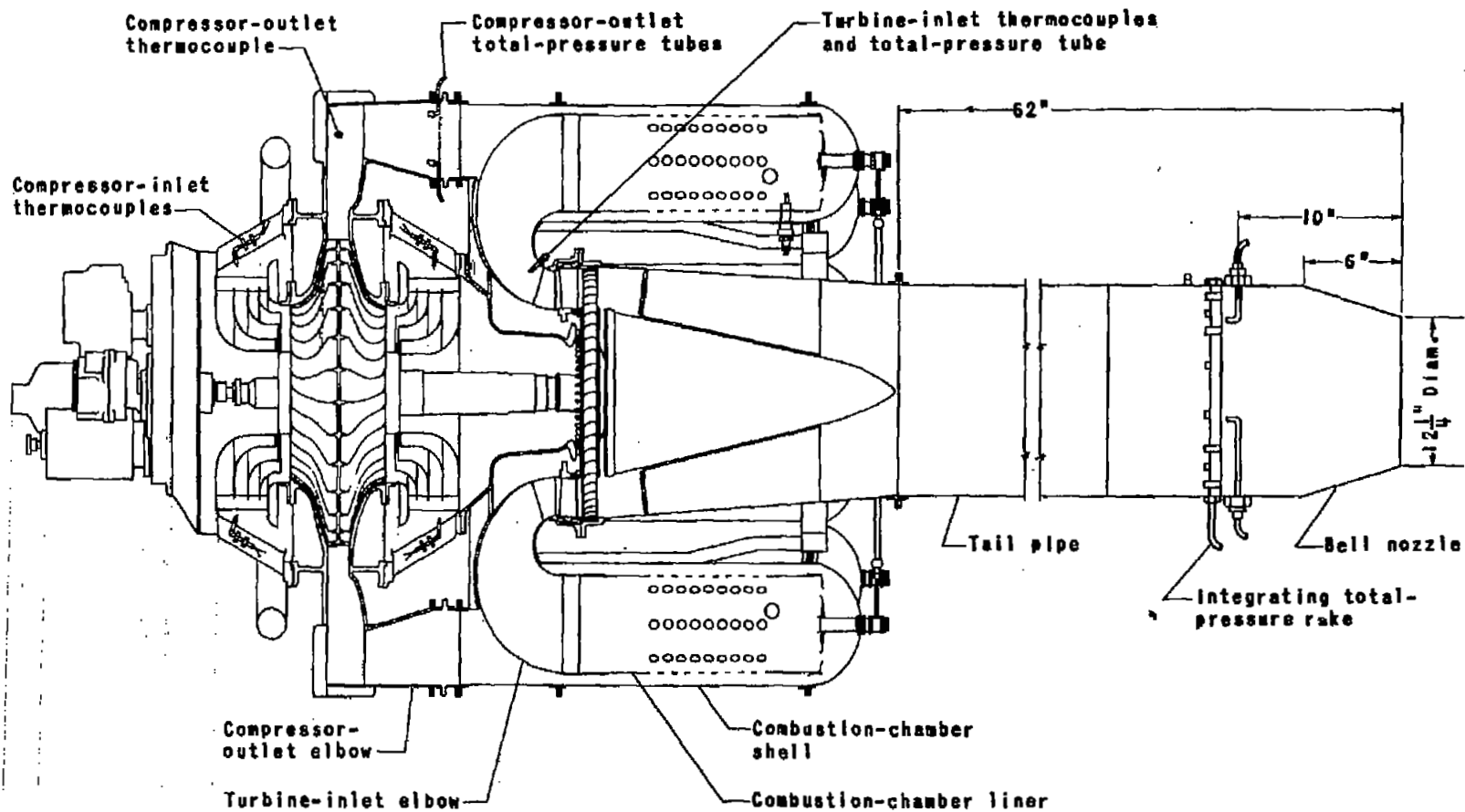
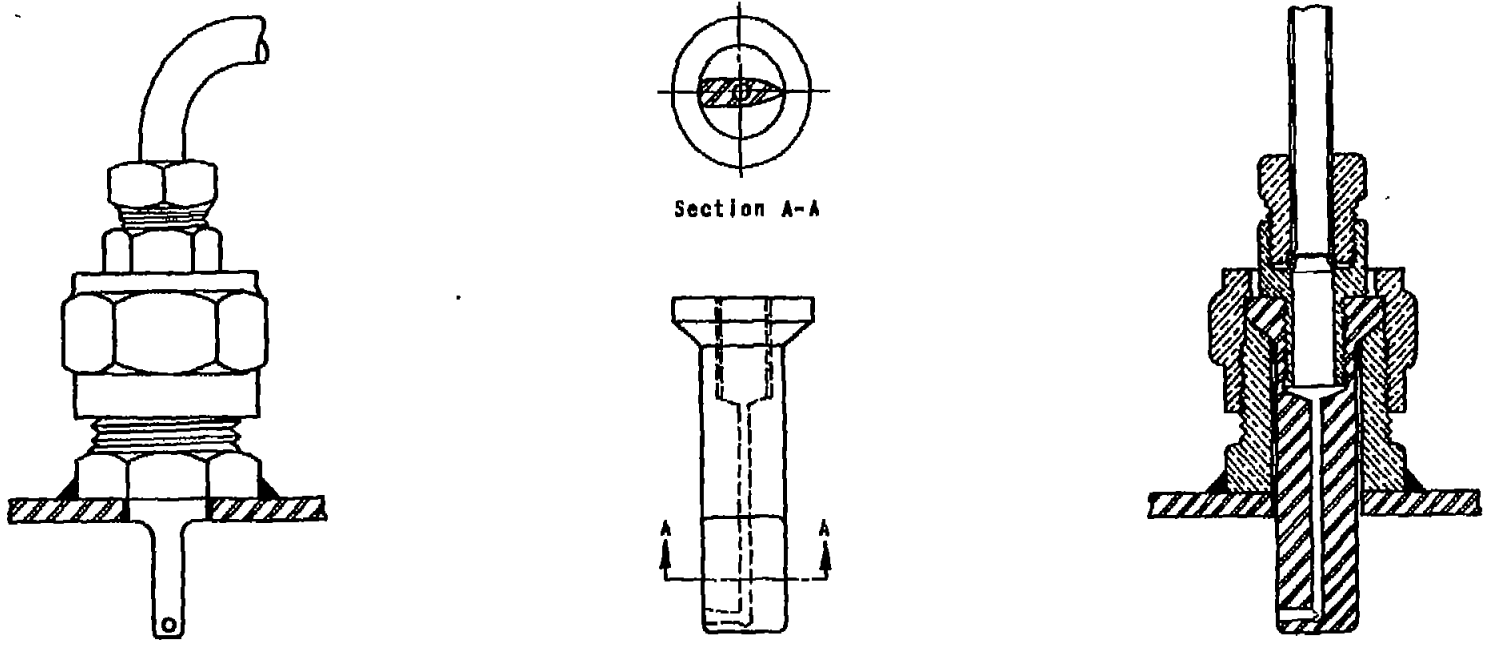


FIG. 2

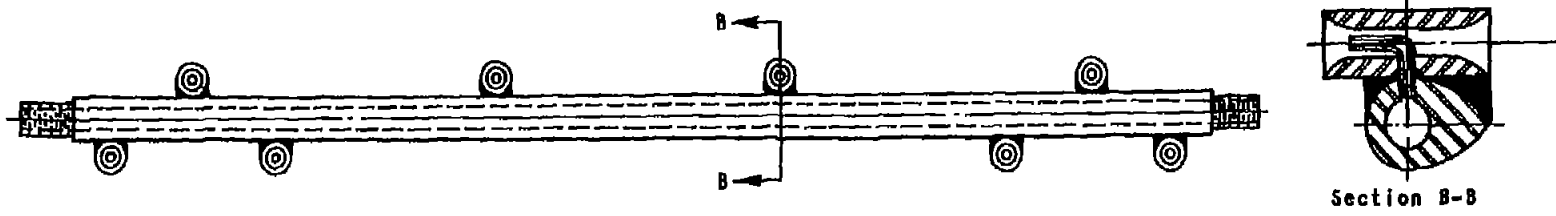
NACA RM No. E7801

Figure 2. - Schematic drawing showing location of pressure tubes and thermocouples in 1-16 jet-propulsion engine.

NATIONAL ADVISORY
COMMITTEE FOR AERONAUTICS

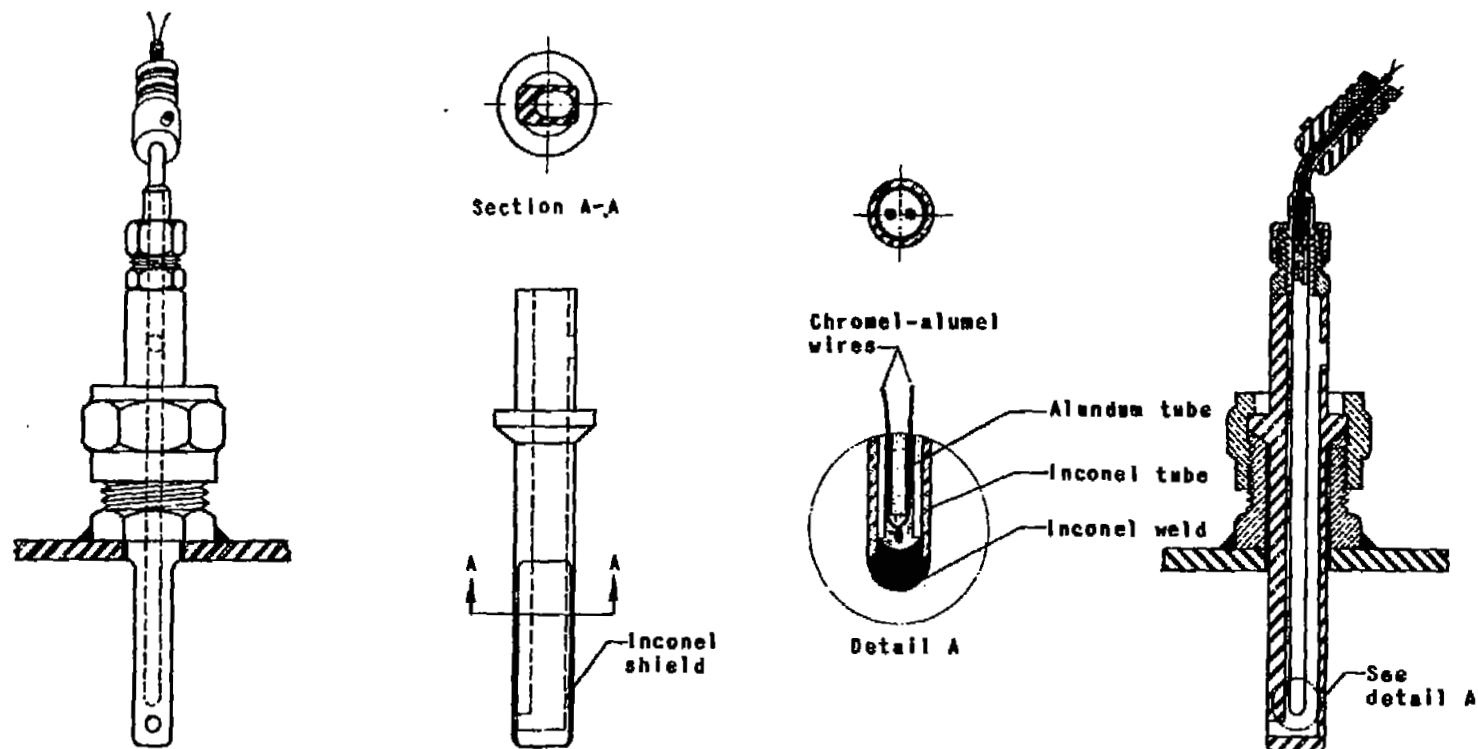


(a) Turbine-inlet total-pressure tube.

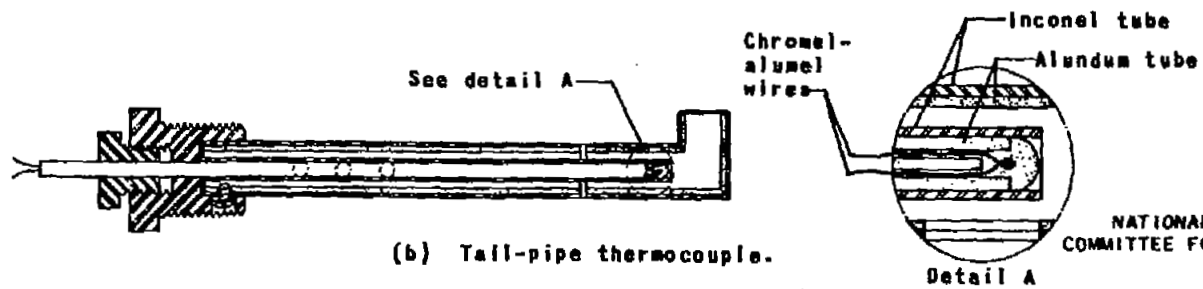


(b) Tail-pipe total-pressure integrating rake.

Figure 3. - Design of total-pressure tubes used in high-temperature, high-velocity gas stream.



(a) Turbine-inlet thermocouple.



(b) Tail-pipe thermocouple.

NATIONAL ADVISORY
COMMITTEE FOR AERONAUTICS

Figure 4. - Design of thermocouples used in high-temperature, high-velocity gas stream.

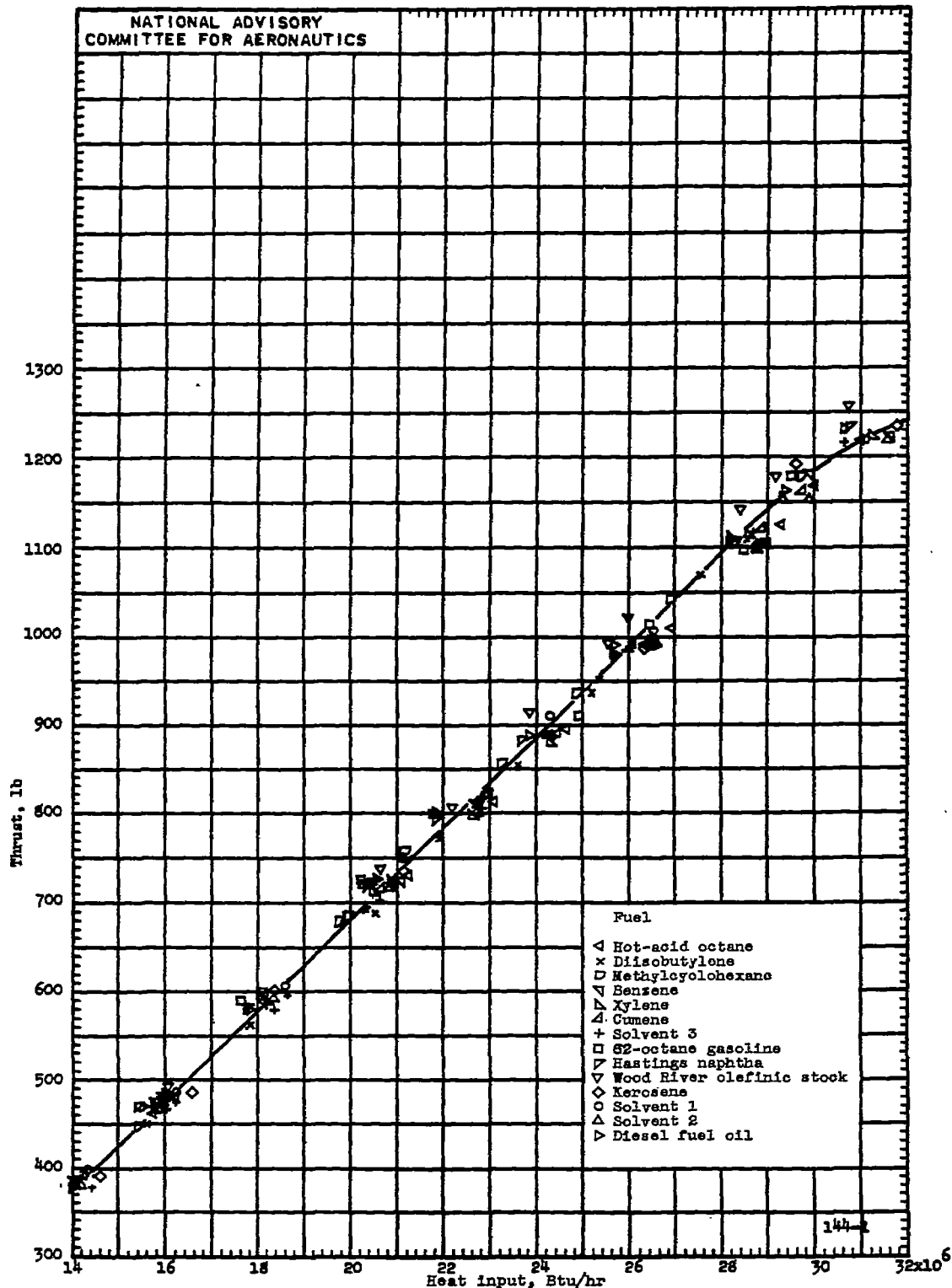


Figure 5. - Variation of thrust with heat input for different fuels at static sea-level conditions. I-16 jet-propulsion engine. Data corrected to standard sea-level conditions.

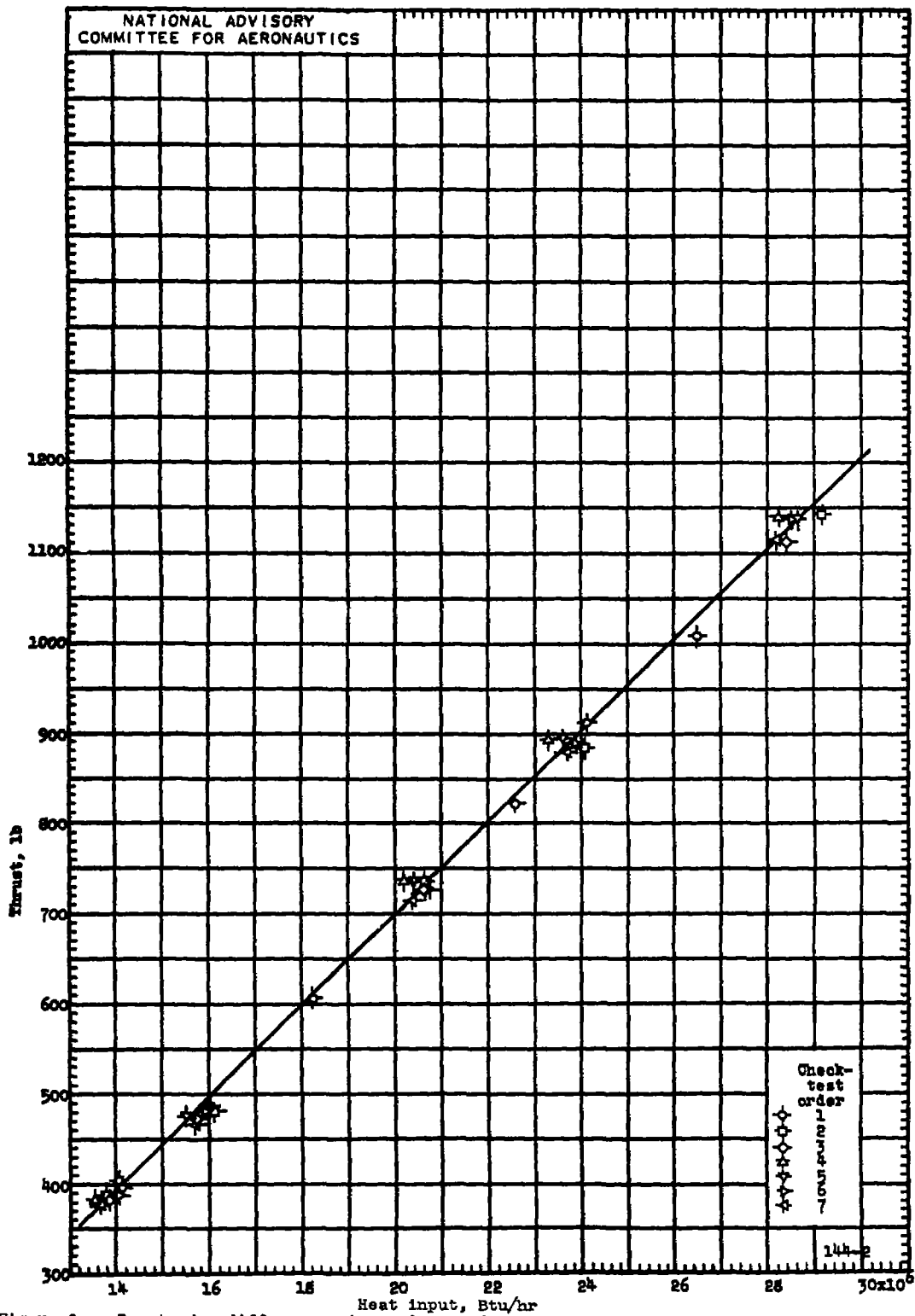


Figure 6. - Day-to-day differences in engine performance over period of test program, using standard reference fuel at static sea-level conditions. I-16 jet-propulsion engine, fuel, solvent 1. Data corrected to standard sea-level conditions.

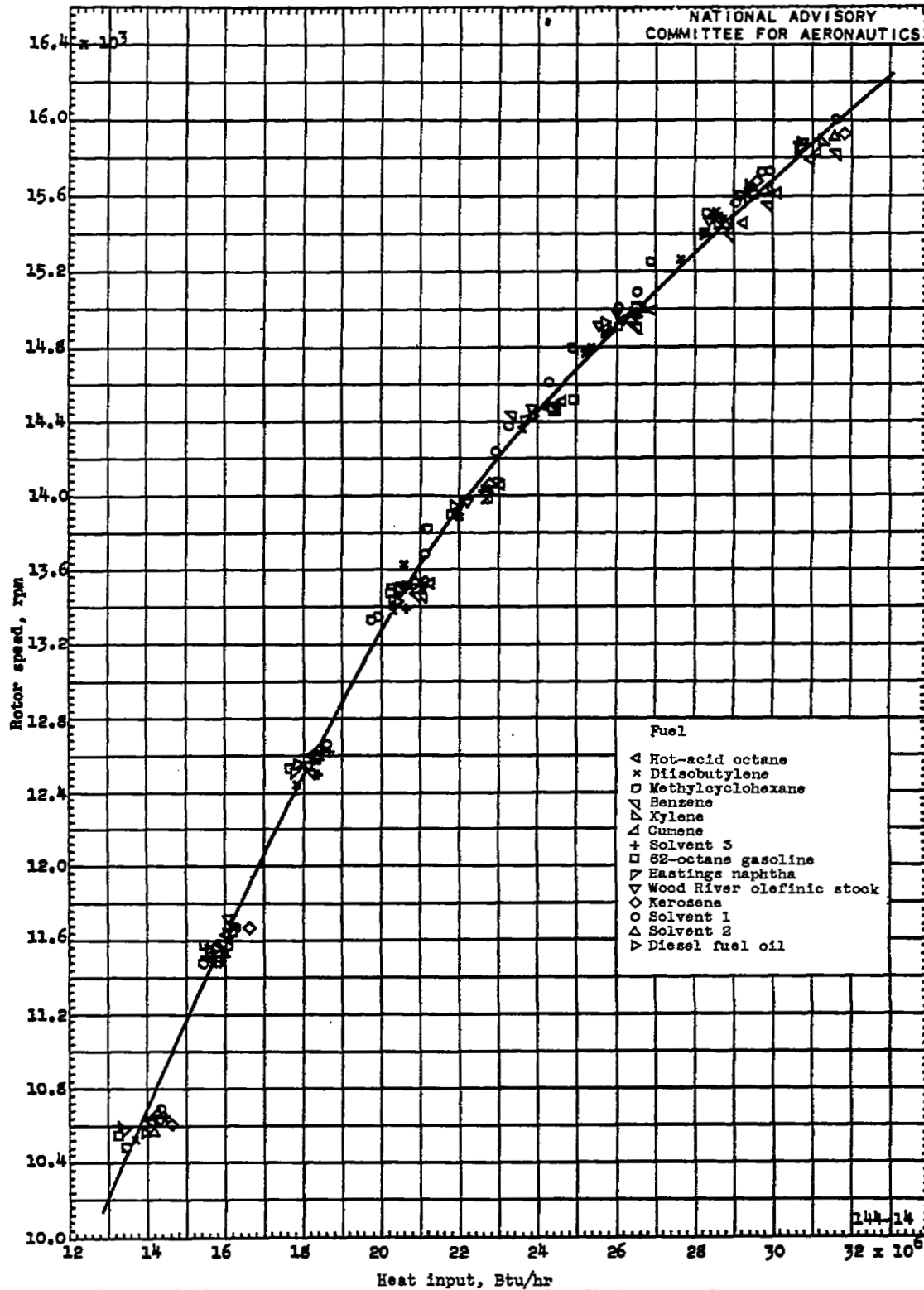


Figure 7. - Variation of rotor speed with heat input for different fuels at static sea-level conditions. I-16 jet-propulsion engine. Data corrected to standard sea-level conditions.

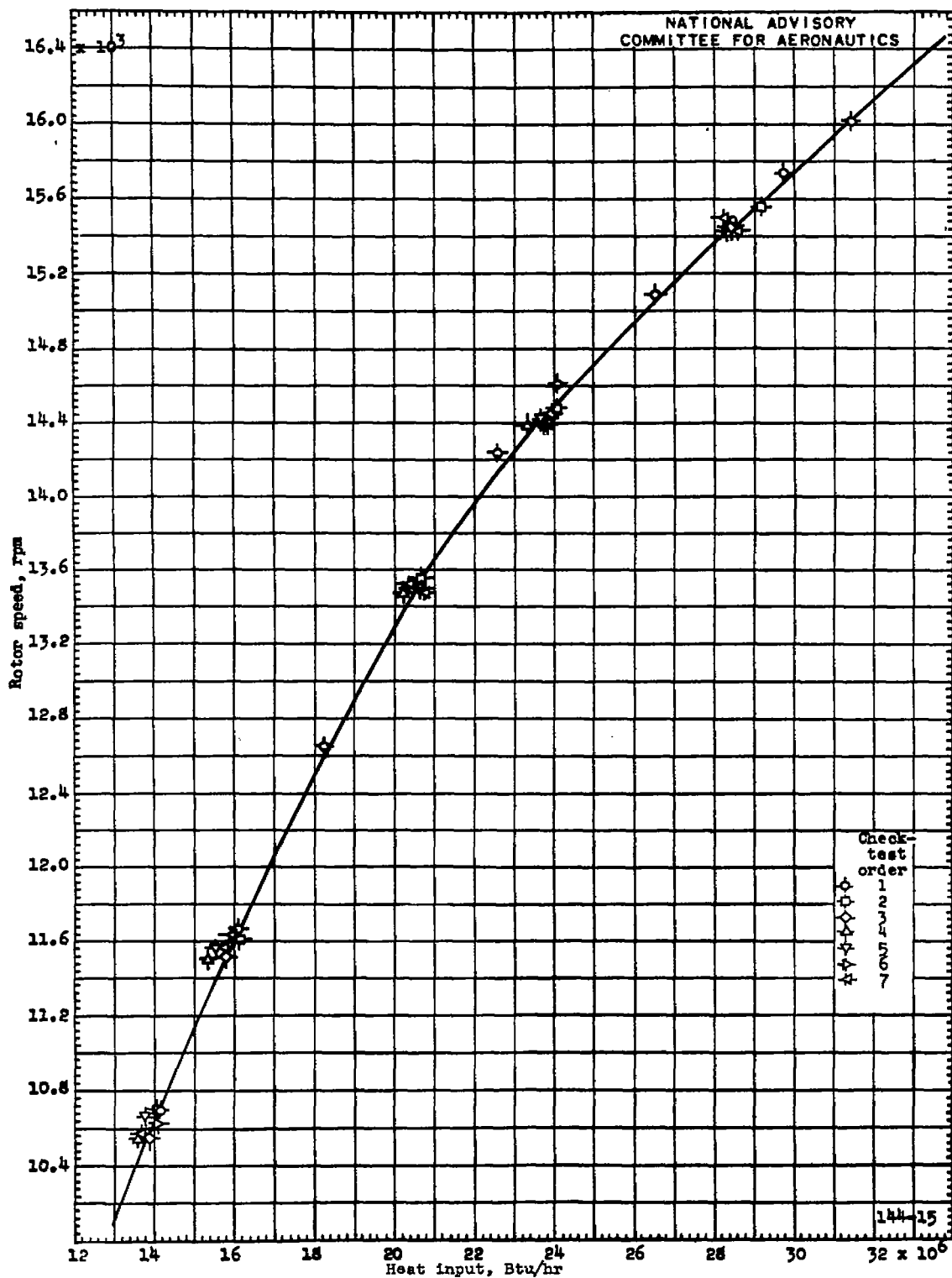


Figure 8. - Day-to-day differences in engine performance over period of test program using standard reference fuel at static sea-level conditions. I-18 jet-propulsion engine; fuel, solvent 1. Data corrected to standard sea-level conditions.

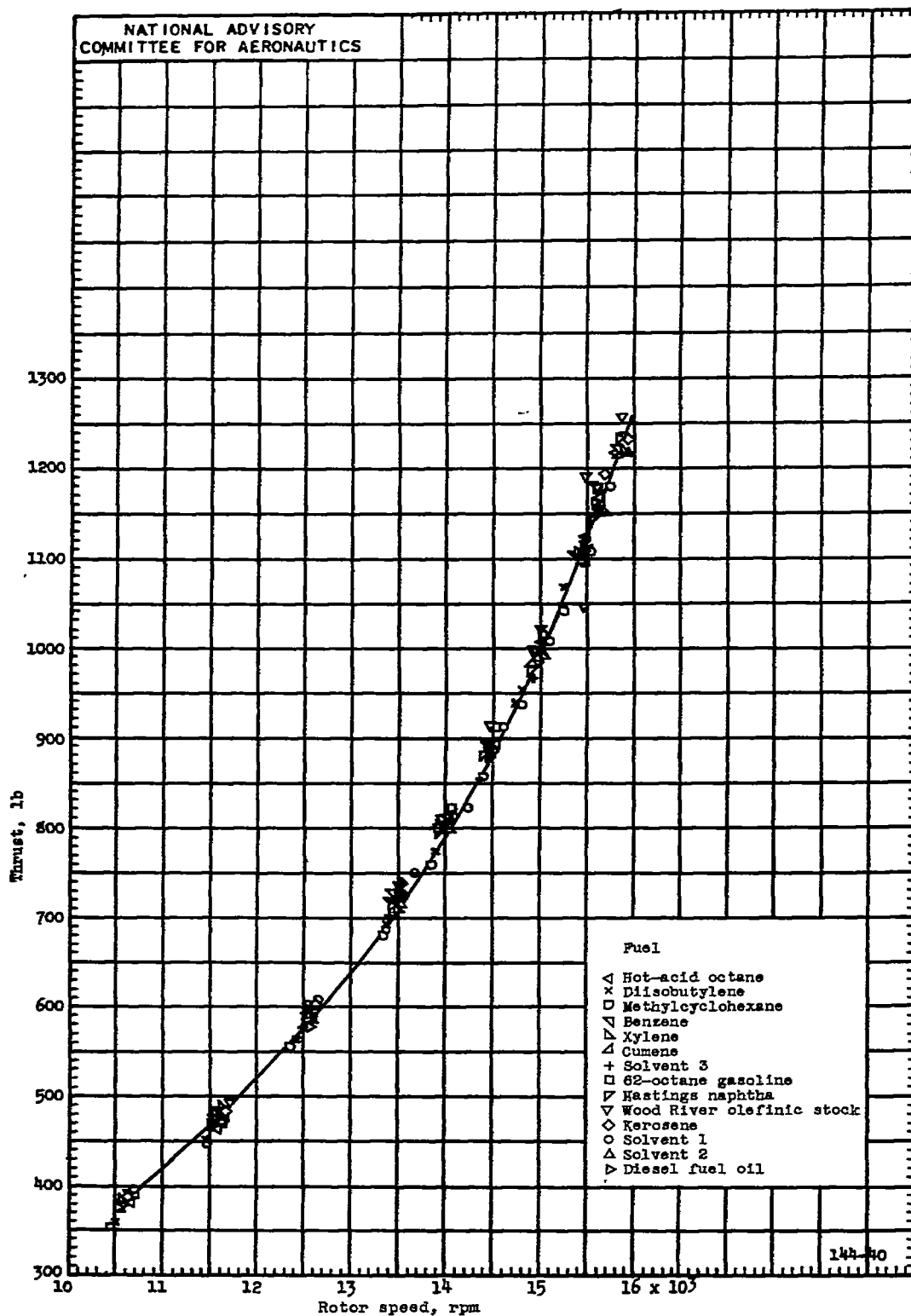


Figure 9. - Variation of thrust with rotor speed for different fuels at static sea-level conditions. I-16 jet-propulsion engine. Data corrected to standard sea-level conditions.

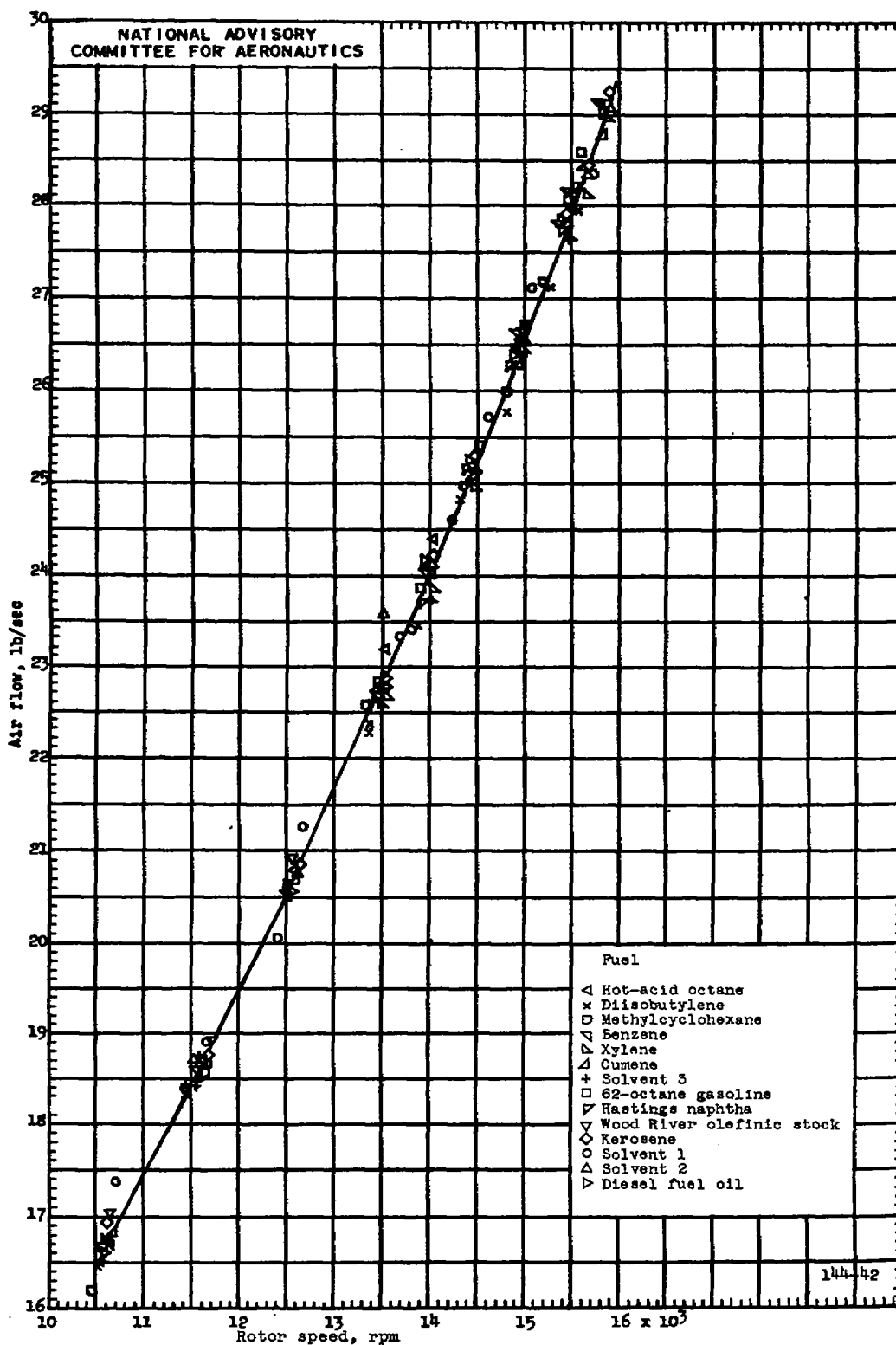


Figure 10. - Variation of air flow with rotor speed for different fuels at static sea-level conditions. I-16 jet-propulsion engine. Data corrected to standard sea-level conditions.

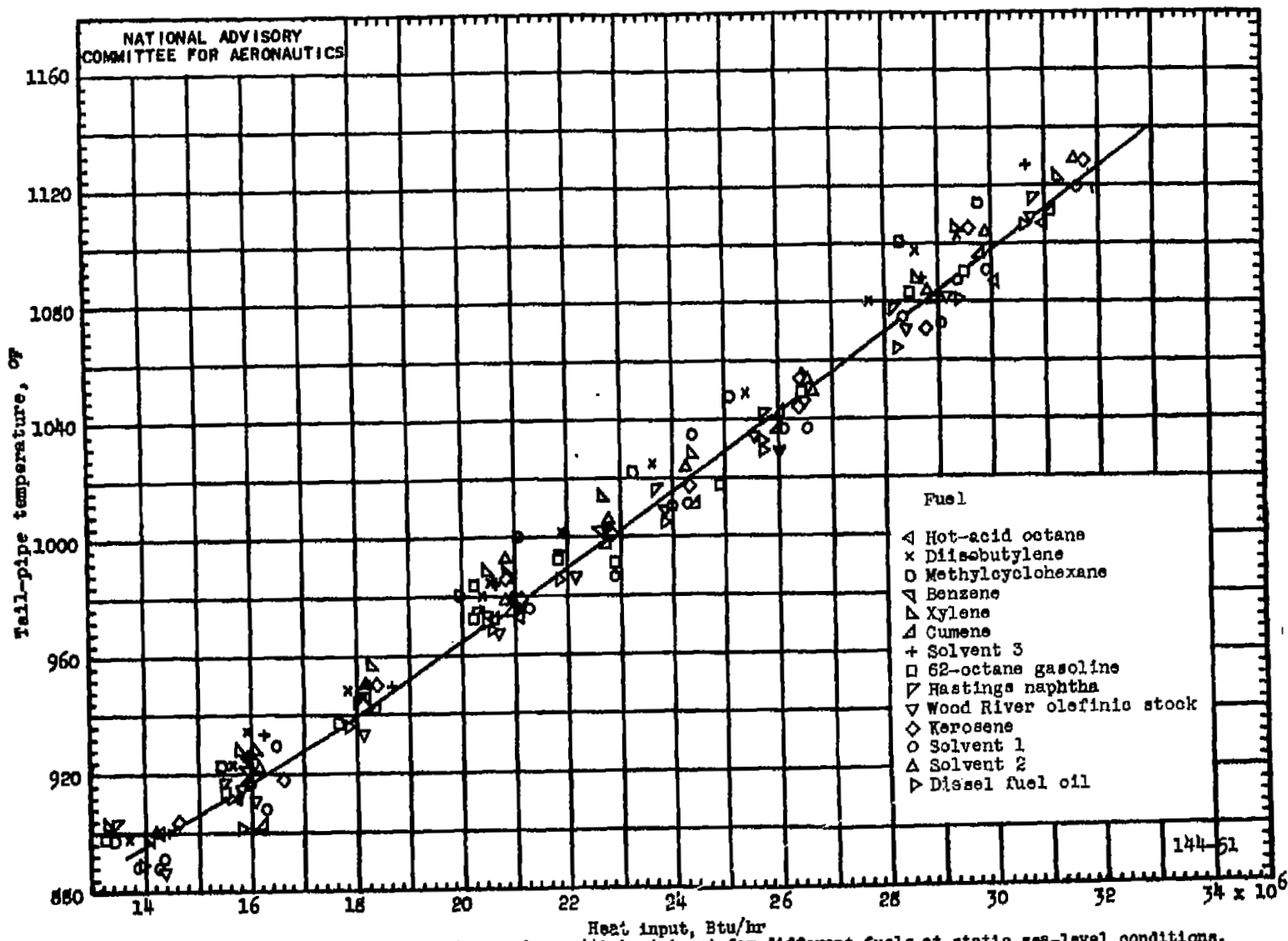


Figure 11. - Variation of tail-pipe temperature with heat input for different fuels at static sea-level conditions. I-16 jet-propulsion engine. Data corrected to standard sea-level conditions.

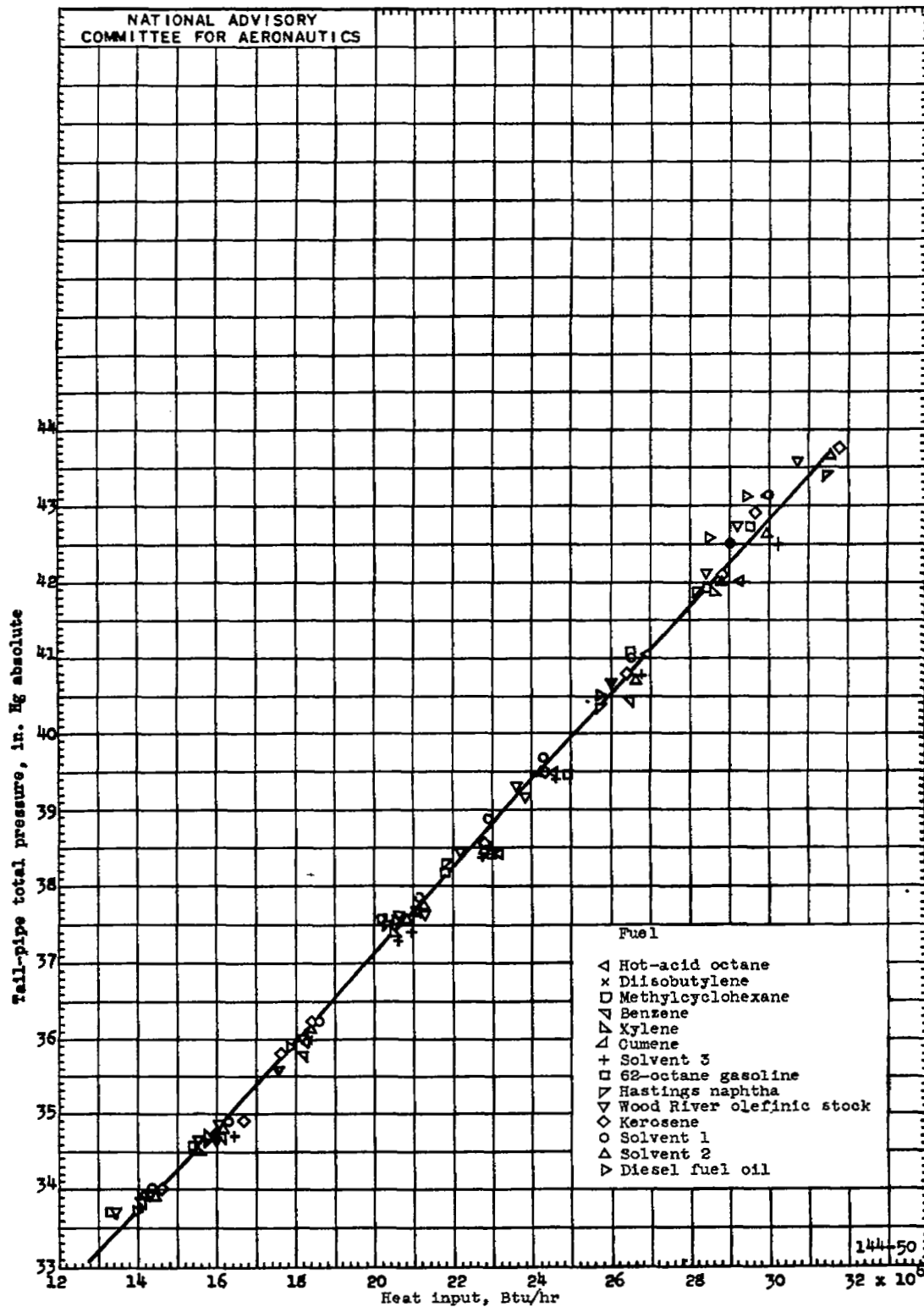


Figure 12. - Variation of tail-pipe total pressure with heat input for different fuels at static sea-level conditions. I-16 jet-propulsion engine. Data corrected to standard sea-level conditions.

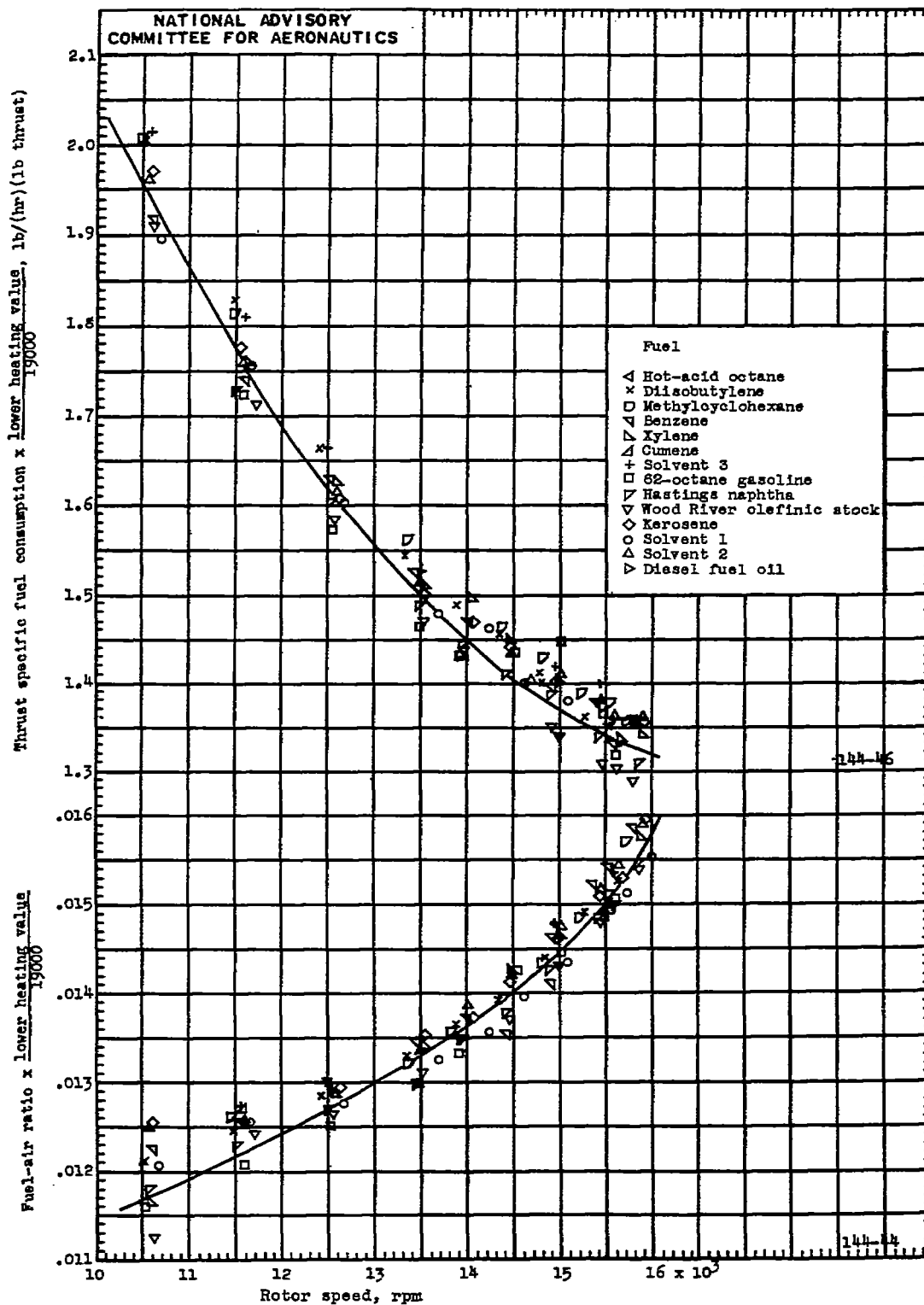


Figure 13. - Variation of thrust specific fuel consumption and of fuel-air ratio with rotor speed at static sea-level conditions for different fuels corrected to a standard lower heating value of 19,000 Btu per pound. I-16 jet-propulsion engine. Data corrected to standard sea-level conditions.

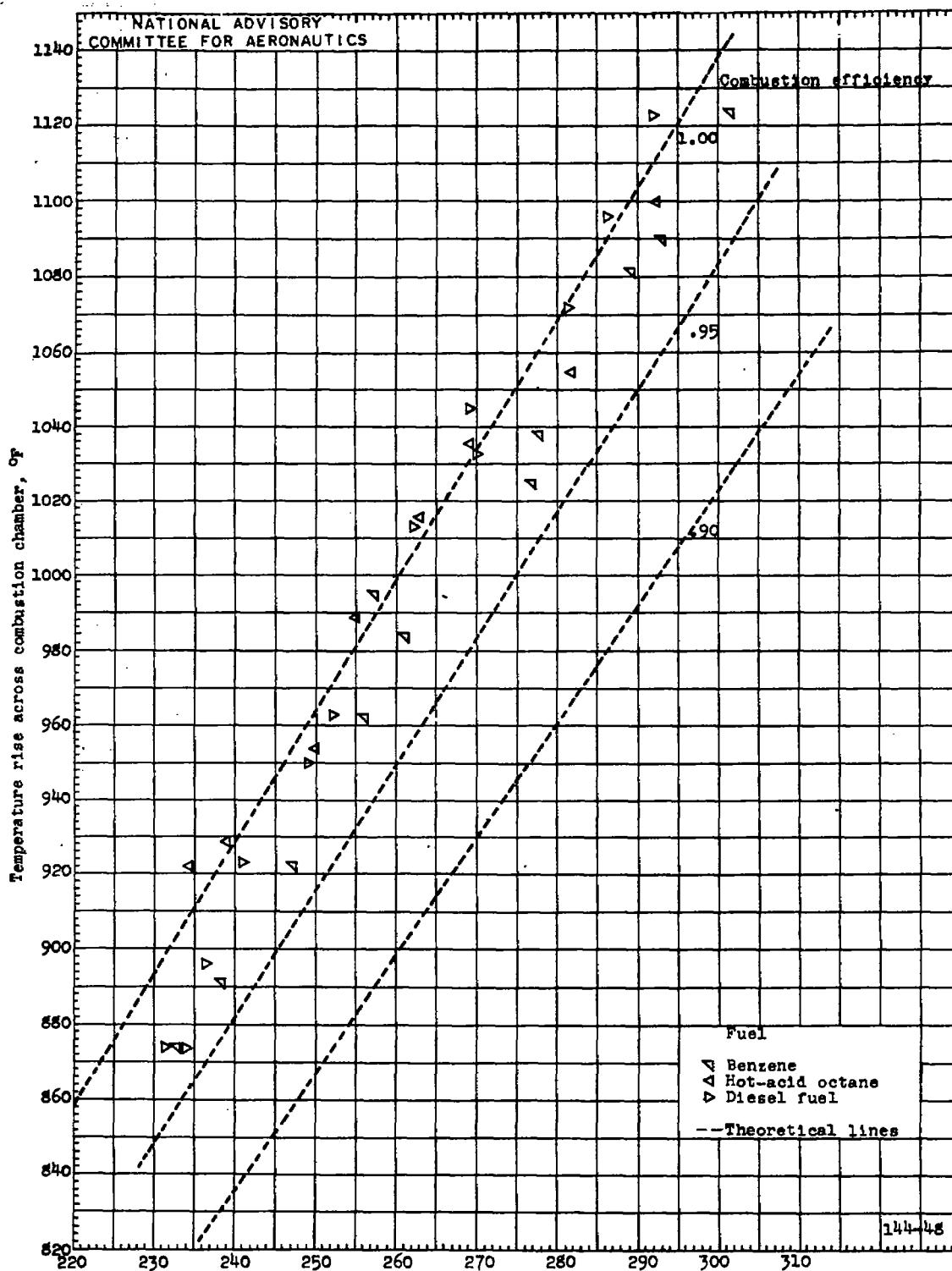


Figure 14. - Combustion efficiency as indicated by temperature rise across combustion chambers at static sea-level conditions. I-16 jet-propulsion engine. Data corrected to standard sea-level conditions.

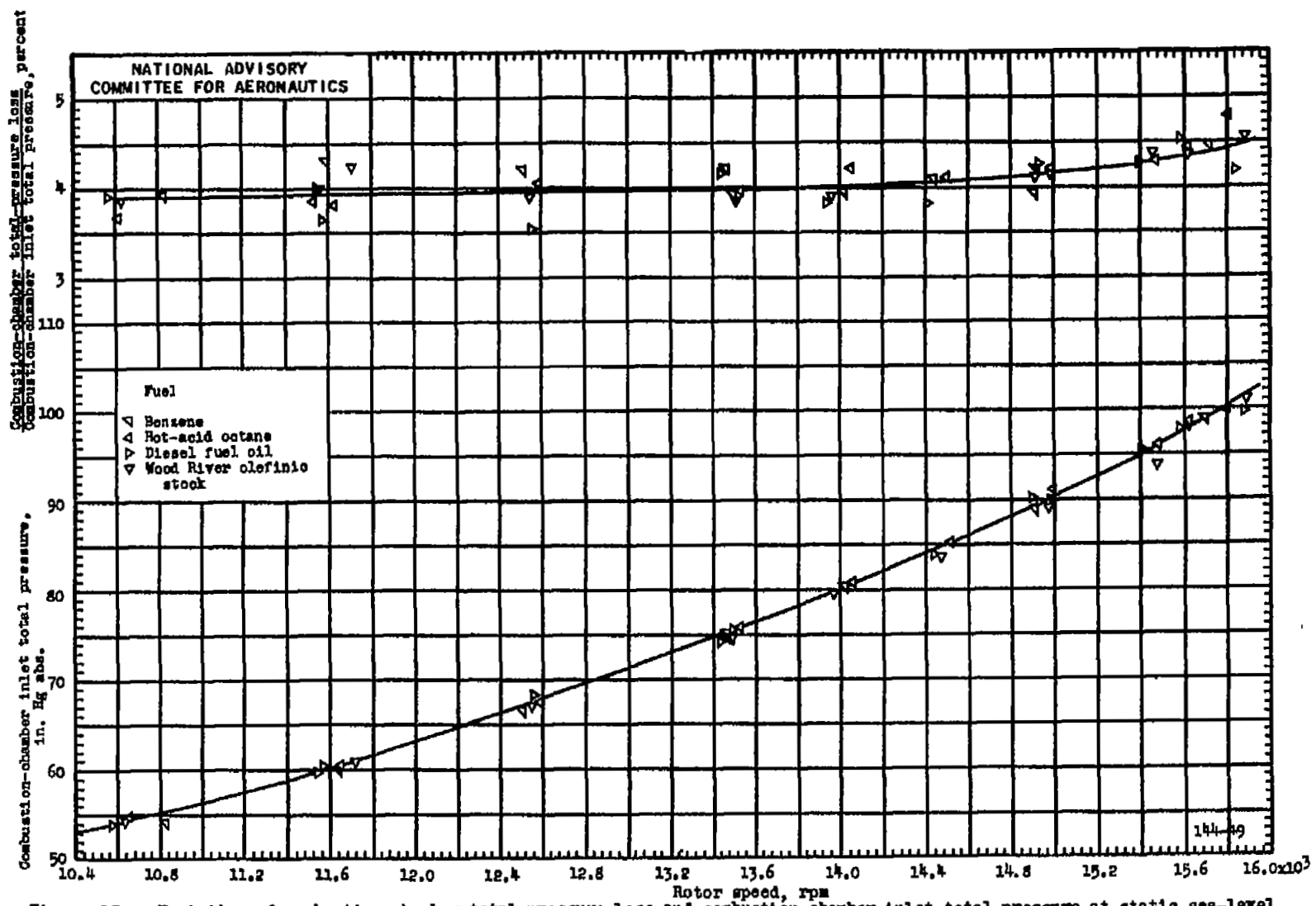


Figure 15. - Variation of combustion-chamber total-pressure loss and combustion-chamber inlet total pressure at static sea-level conditions. I-16 jet-propulsion engine. Data corrected to standard sea-level conditions.

NASA Technical Library



3 1176 01435 0467